Matching of a stripe injection laser to an external resonator

1990 Sov. J. Quantum Electron. 20 704

(http://iopscience.iop.org/0049-1748/20/6/A40)

MIRRORS, RESONATORS

Matching of a stripe injection laser to an external resonator

V. L. Velichanskiĭ, M. V. Zverkov, A. S. Zibrov, V. V. Nikitin, V. A. Sautenkov, N. V. Senkov, V. M. Sitkin, and G. T. Pak

P. N. Lebedev Physics Institute, Academy of Sciences of the USSR, Moscow
(Submitted March 13, 1989; resubmitted December 28, 1989)
Kvantovaya Elektron. (Moscow) **17**, 781–786 (June 1990)

Theoretical and experimental investigations of the characteristics of matching of a planar active waveguide to an external axially symmetric resonator are reported. The dependences of the threshold current on the external resonator length are obtained for stripe injection lasers with the waveguide amplification effect. These dependences are shown to be opposite for a resonator with a parallel beam in the external part and for a system with beam focusing by an external mirror. In the case of lasers with a dispersive external resonator the slopes of the dependences are sensitive to the spectral tuning of a selective element. It is shown that the observed characteristics of the dependences of the threshold pumping rate on the length of the external resonator are related to the change in the curvature of the wavefront of the field during the passage through the external part.

INTRODUCTION

The use of a selective external resonator in an injection semiconductor laser makes it possible to reduce the lasing threshold, widen the tuning range, and reduce by several orders of magnitude the width of the emission line.[1,2] These parameters of an injection laser with an external resonator (ILER) are governed largely by the effectiveness of the external feedback loop.[3,4]

The first discussion of the matching of a planar active laser waveguide to an axially symmetric external resonator was reported in Ref. 5, where the light-emitting face and the external mirror plane were assumed to be located in the focal planes of the same matching objective. In this geometry a Gaussian beam is self-reproduced after a complete round trip in the external resonator and this is true irrespective of the initial parameters of the beam. Changes in a Gaussian beam in the course of a round trip through an external resonator are considered in Ref. 6 as a function of the optical power of the matching objectives and of the distance to the external mirror. In addition to the configuration described in Ref. 5, several more variants have been suggested for ensuring self-reproduction of the wavefront after a round trip in an external resonator. Construction of an external resonator with a concave external mirror, which does not distort the field in the active part of an injection laser, has been reported.

Our aim was to investigate theoretically and experimentally the effectiveness of such external optical coupling as a function of the length and configuration of the external resonator.

1. THEORETICAL ANALYSIS OF MATCHING

In order to optimize matching in respect of the losses and of the value of the threshold current, we must solve a self-consistent problem for the field in a composite spatially inhomogeneous resonator. We shall do this subject to certain simplifying assumptions for injection lasers exhibiting gain-induced confinement of the field.

An analysis of the matching of a laser to an external resonator will be made in two stages. We shall first consider the transformation of a light beam in the external resonator and then discuss changes experienced by the beam inside the active region when a feedback is established. In this analysis we shall use a model of an ILER proposed in Ref. 8, but we shall make the following six assumptions.

1. We shall assume that the thickness of a planar active waveguide $d_x \leqslant 0.5\ \mu$m (along the X axis) is considerably less than the width of a stripe contact $dy \geqslant 5\ \mu$m (along the Y axis) and less than the wavelength $\lambda_0 = 0.8$–$1.3\ \mu$m. We shall postulate that the optical length of the laser is $nl \approx 10^{-3}$ m, which represents only a small fraction of the total external resonator length L ($nl/L \approx 10^{-2}$–10^{-3}).

2. We shall also assume that the field distribution on the face of a laser just after emerging from the semiconductor crystal is Gaussian and it can be described by

$$E(x,y,0) = E_0 \exp\,[-x^2(1/W_x^2 + ik/2R_x) - y^2(1/W_y^2 + ik/2R_y)], \qquad (1)$$

where W_y, R_y and W_x, R_x are the half-widths and radii of curvature of the wavefront of a Gaussian radiation beam in the p-n junction plane (YZ plane) and at right-angles (XZ) to this plane, respectively; $k = 2\pi/\lambda_0$.

3. At right-angles to the active waveguide plane (along the X axis) the distribution of the field in the active region will be assumed to be governed by discontinuities of the refractive index in a double heterostructure and we shall also postulate that changes in the gain can be ignored within these limits because the diffusion length of electrons is considerably longer than the thickness of the active region.

4. The laser mirror facing the external resonator is totally antireflection-coated (its reflection coefficient is zero).

5. None of the optical components of the resonator can give rise to aberrations in the radiation beam. The matching objectives are ideal thin lenses with the optical power $l/f \leqslant \lambda_0/\pi W_x^2$.

6. We shall finally assume that the determination of the characteristic dimensions of an ILER ensuring reproduction of the beam along the X axis can be made using geometric optics. This is justified by the fact that the waveguide thickness is $d_x < \lambda_0$.

We shall employ these assumptions in finding the geometric parameters of an ILER ensuring reproduction of the dimensions of the beam W_x after passing through the external resonator. Then, in an analysis of the propagation of the beam in the YZ plane we shall use the Gaussian approximation for the beam. In the geometric-optics approximation the changes in the distance from the beam to the axis of the system and in the angle of tilt of the beam to the axis are described by the following ray matrix (M):

$$\begin{pmatrix} x' \\ \gamma' \end{pmatrix} = (M)\begin{pmatrix} x \\ \gamma \end{pmatrix} \equiv \begin{pmatrix} A & B \\ C & D \end{pmatrix}\begin{pmatrix} x \\ \gamma \end{pmatrix}. \qquad (2)$$

We shall find more accurately the type of the matrix that describes propagation of a ray in an external resonator ($n = 1$, $\lambda = \lambda_0/n = \lambda_0$). According to the above assumptions, the dimensions of the source and of its image, formed after a complete round trip through the resonator, can be ignored: $x' = x = 0$. Consequently, $x' = A\cdot O + B\cdot\gamma = 0$ applies to any angle, i.e., $B = 0$, but since the determinant of the ray matrix is equal to unity,[7] we obtain $AD = 1$.

Propagation of radiation in the p-n junction plane can be described in the approximation of Gaussian beams specified by the radius of curvature of the wavefront R and by the beam half-width W, which are both determined uniquely by a complex parameter:

$$1/q(z) = 1/R(z) + i\lambda/\pi W^2(z). \qquad (3)$$

In the course of propagation of a Gaussian beam through an optical system this complex parameter varies in accordance with the relationship

$$q_2 = (Aq_1 + B)/(Cq_1 + D), \qquad (4)$$

where A, B, C, and D are the elements of the same matrix (M). If we assume that $B = 0$, we obtain

$$1/R_2 + i\lambda/\pi W_2^2 = C/A + (D/A)(1/R_1 + i\lambda/\pi W_1^2). \qquad (5)$$

Since in this plane the size of the beam should also be self-reproduced after passing through the resonator, it follows that $W_2 = W_1$ and $D = A$. Since $AD = 1$, we find that $A = D = m = \pm 1$. Later, we shall assume the definition $C \equiv P$. Therefore, in the case of an external resonator ensuring self-reproduction of the beam dimensions after one trip through the resonator, we have $(M) = \begin{pmatrix} m & 0 \\ P & m \end{pmatrix}$, and the relationship (5) assumes the following form for the YZ plane:

$$l/q_2 = l/R_1 + i\lambda/\pi W_y^2 + P/m = l/R_2 + i\lambda/\pi W_y^2. \qquad (6)$$

We shall give the values of m and P for the most widely used external resonators shown in Fig. 1. In the case of an external resonator of type I we have $m = -1$, $P = 2(L - 2f)/f^2$, whereas for type II we have $m = 1$, $P = 2(L - 2f)/f^2$, for type III we have $m = 1$, $P = 2(L - 2f)/f^2 - 2(L - 2f)^2/\rho f^2$, and for type IV we find that $m = 1$, $P = 2(L - 2f - 2F)f^2$, where f and F are the focal lengths of the matching objetives, and ρ is the radius of curvature of the external mirror; $f \ll L$.

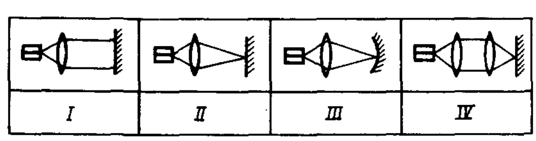

FIG. 1. Different ways of matching an injection laser to an external resonator.

It is clear from Eq. (6) that the wavefront curvature changes by mP in one round trip through the external resonator, and this defines the physical meaning of the parameter P. If $P = 0$, a Gaussian beam returns to the active region without distortion.[6] At first sight it might seem that the losses and the threshold current should be minimal for a resonator with the curvature parameter $P = 0$. However, the mismatch between the wavefronts of the mode emitted by the active waveguide and of the wave returning from the external reflector may be accompanied by an increase in the amplification efficiency if we allow for the spatial distribution of the gain, which should affect the change in the threshold current.

In determination of the lasing threshold of an ILER within the framework of this model we have to replace an antireflection-coated face of a semiconductor crystal with a mirror characterized by a reflection coefficient $r = I_2/I_1$ and by a curvature $P_1 = P/nm$ in the YZ plane. Here, I_1 is the power of the radiation emitted by the laser in the direction of the external resonator and I_2 is the power returned to the active medium.

We shall now report estimates for lasers in which the field is confined to the *p-n* junction plane by the waveguide amplification effect and we shall assume that the gain profile is parabolic:

$$g' = g_0 - {}^1/_2 g_2 y^2 - \alpha, \tag{7}$$

where g_0 is the gain amplitude on the waveguide axis and α represents the distributed losses.

In an active waveguide with the parameters defined by Eq. (7) a Gaussian beam with the complex parameter q_1 changes during the propagation along the Z axis in accordance with the law:[11]

$$\frac{1}{q(z)} = \frac{1}{q_m} \frac{(q_1+q_m)-(q_1-q_m)\exp[2(i-1)z/R_m]}{(q_1+q_m)+(q_1-q_m)\exp[2(i-1)z/R_m]}. \tag{8}$$

Here, q_m is a complex parameter of a steady-state beam established in a waveguide characterized by the parameters

$$R_m = 2(\pi/g_2\lambda)^{1/2}, \quad W_m^2 = 2(\lambda/\pi g_2)^{1/2}. \tag{9}$$

If we assume that the steady-state current is little disturbed by return of the radiation from the external resonator (this can be expressed in the form of condition $|q(0) - q_m)/(q(0) + q_m)| \ll 1$), it is found that Eq. (8) yields

$$W_y^2(z) = W_m^2 \left| 1 + \frac{\pi W_m^2}{\lambda} \frac{P}{mn} \sin\frac{2z}{R_m} \exp\left(-\frac{2z}{R_m}\right) \right|, \tag{10}$$

$$\frac{n}{R_y(z)} = \frac{n}{R_m} + \frac{P}{mn} \cos\frac{2z}{R_m} \exp\left(-\frac{2z}{R_m}\right). \tag{11}$$

It follows from the above relationships that the beam halfwidth $W_y(z)$ and the radius of curvature of the wavefront $R_y(z)$ exhibit damped oscillations approaching the values W_m and R_m typical of a waveguide at a distance $\Delta z \approx R_m$.

If the results are averaged in the XY plane along the Z axis of the active region, the effective power gain is

$$g(z) = \frac{\iint |E(x,y,z)|^2 2g'(x,y,z)\,dx\,dy}{\iint |E(x,y,z)|^2 dx\,dy}, \tag{12}$$

where $E(x,y,z)$ is the field at the point x, y, z; $2g'(x,y,z)$ is the local gain at this point. Substituting in Eq. (12) the expressions for the field (1) and the gain (7), and separating the variables, we find that direct integration yields

$$g(z) = 2(g_0 - \alpha - {}^1/_8 g_2 W_y^2(z)) = 2\left(g_0 - \alpha - \frac{\pi}{2\lambda R_m^2} W_y^2(z)\right). \tag{13}$$

If $R_m < l$, where l is the length of the active medium, it follows that the gain achieved in a round trip through the resonator is

$$G = 2l(2g_0 - 2\alpha - 1/R_m - R_m P/8lmn). \tag{14}$$

If we use the threshold condition $r_0 r \exp G = 1$, where r_0 is the reflection coefficient of the injection laser mirror, and the relationship $g_0 = \beta(j - j_0)$, where β is the gain factor, j is the current density, and j_0 is the current density at which resonant absorption vanishes, we can obtain an expression for the threshold current density ($I \propto j_{th}$):

$$I \sim 2j_0\beta + 2\alpha + (2l)^{-1}\ln(r_0 r)^{-1} + 1/R_m + R_m P/8lnm. \tag{15}$$

The first three terms, typical of any resonator, are the components of the pump current density necessary to achieve the population inversion threshold and for the compensation of the internal and external losses, respectively. The term $1/R_m$ represents the usual diffraction losses. The last term, proportional to the curvature parameter P/m, reflects the dependence of the threshold current on the external resonator length. The data given above for m and P show that if the condition $L > f$ satisfied in our experiments is assumed, then $P \propto L$ for type I and II resonators. Therefore, in the case of an ILER of type I ($P/m < 0$) the threshold current should decrease on increase in L, whereas for a type II laser ($P/m > 0$) it should increase.

2. EXPERIMENTAL RESULTS AND DISCUSSION

We used the apparatus shown schematically in Fig. 2. The active region of a laser was matched to an external mirror by a microobjective with a numerical aperture of 0.65 and a focal length of $f = 6.2$ mm. This microobjective was supported by a piezoelectric ceramic plate, which made it possible to vary continuously the position of this objective within 50 μm. The output radiation was directed to a photodiode in order to record the watt-ampere characteristic of the laser, to a diffraction grating 6, and a television monitor 7, which was used to display the emission spectrum; it was also directed to a slit with a photodiode in order to determine the distributions of the radiation in the far- and near-field zones.

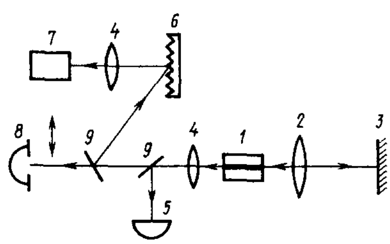

FIG. 2. Experimental setup: 1) injection laser; 2) matching objective; 3) external mirror; 4) objective; 5) photodiode; 6) diffraction grating; 7) television monitor; 8) photodiode with a slit stop; 9) semitransparent mirror.

Figure 1 shows different types of external resonators. The method of organization of the coupling to an external mirror allows us to divide them into two groups: external resonators with "parallel" (types I and IV) and "converging" (types II and III) beams reaching the external mirror. The most widely used matching geometry employs the parallel beam configuration and it is convenient when Fabry–Perot interferometers and diffraction gratings are used as the selective elements. The configuration with a converging beam is less sensitive to angular misalignment of the external mirror than the configuration with a parallel beam. Type IV lasers combine the advantages of both resonator groups, but two high-quality objectives have to be used. We limited our analysis to two most widely used external resonators of type I and II.

When a parallel beam was used a microobjective in an external resonator was aligned so that the beam dimensions changed as little as possible during propagation and this was followed by placing of the other components of the external resonator. Light was reflected by this resonator back to the active region of the laser and a piezoelectric ceramic support was used to set the microobjective at the position ensuring the optimal coupling. The next stage was determination of the dependence of the threshold current on the external resonator length for a fixed position of the microobjective.

We selected the optimal position of the microobjective for each value of L when working with a converging beam. The threshold current was deduced from a kink in the watt-ampere characteristic. For our ILER the kink was sharp and the error in the determination of the threshold current did not exceed 1%. In the case of a laser without an external resonator, the watt-ampere characteristic was smooth and the face of the crystal was not antireflection-coated, so that the threshold could be determined only to within 5%. However, this error (in the determination of the laser threshold in the absence of an external resonator) shifted the dependences without altering their nature. The temperature dependence of the threshold current was ignored (because of reduction in the losses).

The distortions of the field in the waveguide plane because of the self-focusing effect[12] were avoided by recording the spatial characteristics of the radiation at a constant and fairly low radiation power (when the threshold was exceeded by no more than 10%).

We investigated the following types of AlGaAs ($\lambda_0 = 0.78$–0.88 μm) lasers, operating continuously at room temperature: the simplest stripe double heterostructure lasers with a shallow mesa structure and separate optical and electron confinement. The main results were obtained for lasers without lateral confinement. Use was made of lasers with a near-Gaussian field distribution. Samples with the output radiation divergence independent of external feedback were selected. Therefore, we monitored that the condition $l > R_m$ was satisfied, i.e., that the spatial oscillations of the beam emerging from the external resonator were damped out within the active region of the investigated samples.

Figure 3 shows the dependence of the ratio of the threshold current obtained for a lser without an external resonator to the threshold current of an ILER ($I_0/I_{\rm ER}$) for type I and II resonators. Clearly, for a type I resonator the value of $I_{\rm ER}$ decreased on increase in L, whereas for a type II

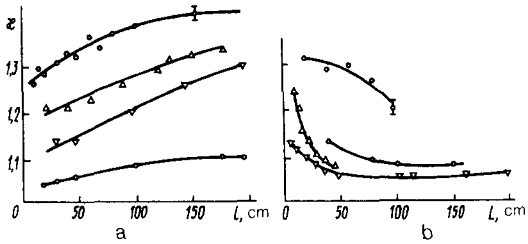

FIG. 3. Dependence of the ratio $\varkappa = I_0/I_{\rm ER}$ of the threshold currents of a laser without an external resonator (coupling) and with an external resonator on the length of this resonator L, obtained for injection lasers of types I (a) and II (b): ●), ∇), △) lasers with a shallow mesa structure; ○) double-heterostructure laser with a stripe contact.

resonator it increased. Figure 3 gives the results only for four lasers, but the experiments were carried out on a large number of lasers (in excess of 40). It should be stressed that the detailed behavior of these curves differed greatly from one laser to another (for example, in the case of stripe-contact lasers the scatter of the curves was as large as in the case of mesa stripe lasers): there was no regular dependence of the derivative of these curves (with respect to the length) on the resonator length. The only common property was an increase in the threshold current in the former case and a fall in the latter. Therefore, the nature of the dependences was in agreement with the results of the above analysis. The scatter of the curves in Fig. 3 was clearly associated with the different internal losses and different dimensions of the active region of a specific laser.

These results were true not only of the threshold, but also of other characteristics of these lasers. When the pump current exceeded slightly the threshold, so that the strong nonlinearities of the watt-ampere characteristics were not yet manifested, a change in the power at a fixed value of the current above the threshold represented a change in the coupling efficiency, also plotted in Fig. 3. For example, for a type I laser an increase in L in the range from 10 cm to 1.5 m increased the output radiation power by 5–15%.

A variant in which the function of an external mirror is poerformed by a selective element (diffraction grating or holographic selector) is of considerable practical interest in spectroscopy and metrology. Figure 4 shows the dependences of the reduced threshold current on the length of the external resonator in the case of a stripe double-heterostructure laser obtained for different alignments of the diffraction grating. In one case the laser was tuned to the center of the gain profile and in the other two cases it was tuned to the wings of the line at points separated by ± 2 nm from the center. Clearly, the slopes of the curves decreased on increase in the tuning frequency of the selective element.

We shall now consider and analyze the results obtained using a diffraction grating as an external reflector and we shall do this on the basis of Eq. (15). Figure 5a gives the qualitative frequency dependences of the gain for various nonequilibrium carrier densities. Assuming that the nonequilibrium carrier density profile in the active region along the Y axis was parabolic (Fig. 5b), we found the distribution of the gain in the active medium at three lasing frequencies (corresponding to three positions of the diffraction grating), shown in Fig. 5c. It is clear from this figure that the effective width of the active region of the laser was always less in the

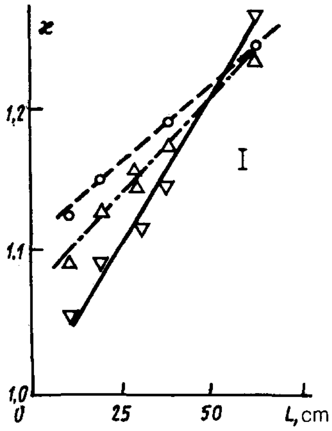

FIG. 4. Dependence $\varkappa(L)$ obtained using a plane diffraction grating as a mirror. The continuous curve represents the emission of radiation in the long-wavelength wing of the gain profile; the dashed curve represents lasing in the short-wavelength wing; the chain curve represents lasing at the center of the gain profile.

short-wavelength part of the gain profile. When the diffraction grating was tuned to wavelengths longer than the center of the gain profile, the effective width of the active region of the laser increased. This increase should increase the slope of the dependences of the threshold current on L [because $R_m \propto W_m$ in Eq. (15)—see also Eq. (9)], as was indeed observed experimentally. Naturally, when the diffraction grating was detuned away from the center of the gain profile, there was a change not only in the slope of the dependence of $\varkappa$ on L, but also in the gain itself.

The most restrictive assumption in the above model of an ILER is that the surface of the laser facing the external resonator is totally antireflection-coated. However, in our

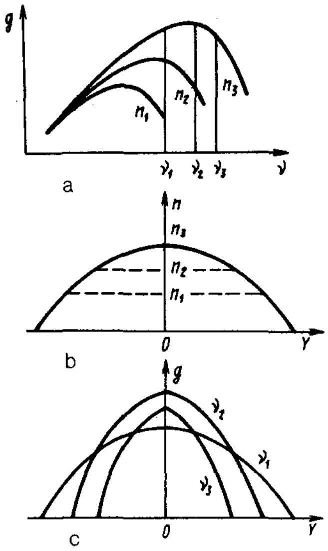

FIG. 5. a) Spectral contour of the gain g plotted for different carrier densities n in the middle of an active waveguide of a laser ($y = 0$, $n_1 < n_2 < n_3$). b) Distribution of the carrier density in the plane of the waveguide. c) Distributions of the gain in the plane of the waveguide, for a fixed pump current in an injection laser with an external resonator, at the center of the gain profile (ν_2), and in the long-wavelength (ν_1) and short-wavelength (ν_3) wings.

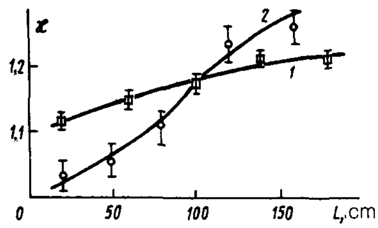

FIG. 6. Dependence $\varkappa(L)$ for an injection laser with a shallow mesa structure before (1) and after (2) antireflection coating.

experiments we investigated lasers which were completely or partly free of antireflection coatings. A detailed analysis carried out allowing for the interference between the wave emitted by the laser and that returning from the external resonator would be quite difficult. We therefore investigated the influence of an antireflection coating on the dependence of the threshold current on the external resonator length in the following experiment. We recorded the dependence of the threshold current on the external resonator length for several double-heterostructure lasers with a shallow mesa structure. These lasers were then antireflection-coated and the dependences were recorded again (Fig. 6). We found that the dependence of the threshold current on the external resonator length was strongest for antireflection-coated lasers. The value of $\varkappa$ varied within wider limits: from 1.03 to 1.3 (before antireflection coating, the range was 1.1–1.2). As expected, the reflection of light from the surface of the laser facing the external resonator weakened the influence of the external mirror. In fact, an increase in the reflection coefficient of an intermediate mirror reduced the relative change in the losses due to a change in L. In spite of this, the dependence $\varkappa$ (L) remained the same.

We also studied lasers with partial lateral confinement. For the majority of them the slopes of the dependences $\varkappa(L)$ were less than for lasers without such confinements, but in some cases there were no regular dependences. Clearly, this was due to the fact that the attenuation length of the returned wave in the active region with lateral confinement was considerably longer than the period of oscillations of its constriction. Therefore, an increase in the effective gain on compression of the field toward the axis of the stripe, where the gain was higher, and its reduction during the subsequent penetration of the field into the regions where the absorption predominated, balanced each other out in averaging over the resonator length.

A study of the emission spectra of ILERs showed that the use of a nonselective type II external resonator sometimes widened the range of single-frequency emission (particularly when the external resonator was short).[6]

It should be pointed out that the curvature of the field wavefront in the active region of the laser could be modified also by other methods. In the experiments reported in Refs. 8 and 9 one of the resonator mirrors was made cylindrical (with the center of curature outside the active region), so that the laser resonator became unstable. This resulted in the emission of a single longitudinal mode. A theoretical analysis of a laser with curved mirrors was made in Ref. 10. The exact solutions of the wave equations were obtained, but only lasers with lateral confinement were considered.

CONCLUSIONS

We investigated experimentally and theoretically the influence of the geometry of an external resonator on the efficiency of matching to stripe injection lasers. We found that the threshold current and the output radiation power depended on the length of the external resonator and the slopes of these dependences (positive or negative) were determined by the matching configuration. These relationships were manifested even more strongly by antireflection-coated lasers. A change in the slope of the dependences on the spectral tuning of a dispersive element was observed for selective injection lasers with an external resonator. These results were explained by a change in the curvature of the radiation wavefront during one round trip through the external resonator.

In the case of stripe lasers in which the field is gain-confined, the lasing threshold could be reduced and the efficiency of the external coupling could be imporved by using external resonators characterized by $P/m<0$.

The authors are grateful to A. P. Bogatov for valuable discussions.

[1]A. M. Akul'shin, N. G. Basov, V. L. Velichanskiĭ *et al.*, Kvantovaya Elektron. (Moscow) **10**, 1527 (1983) [Sov. J. Quantum Electron. **13**, 1003 (1983)].

[2]V. L. Velichanskiĭ, A. S. Zibrov, V. I. Molochev *et al.*, Kvantovaya Elektron. (Moscow) **8**, 1925 (1981) [Sov. J. Quantum Electron. **11**, 1165 (1981)].

[3]É. M. Belenov, V. L. Velichanskiĭ, A. S. Zibrov *et al.*, Kvantovaya Elektron. (Moscow) **10** 1232 (1983) [Sov. J. Quantum Electron. **13**, 792 (1983)].

[4]O. Nilsson, S. Saito, and Y. Yamamoto, Electron. Lett. **17**, 589 (1981).

[5]E. M. Phillip-Rutz and H. D. Edmonds, Appl. Opt. **8**, 1859 (1969).

[6]A. M. Akul'shin, V. I. Borodulin *et al.*, Preprint No. 157 [in Russian], Lebedev Physics Institute, Moscow (1982).

[7]A. Gerrard and J. M. Burch, *Introduction to Matrix Methods in Optics*, Wiley, New York (1975).

[8]A. P. Bogatov, P. G. Eliseev, M. A. Man'ko *et al.*, Kvantovaya Elektron. (Moscow) **7**, 1089 (1980) [Sov. J. Quantum Electron. **10**, 620 (1980)].

[9]R. R. Craig, L. W. Casperson, O. M. Stafsudd *et al.*, Electron Lett. **21**, 62 (1985); J. Salzman, T. Venkatesan, R. Lang, M. Mittelstein, and A. Yariv, Appl. Phys. Lett. **46**, 218 (1985).

[10]R. J. Lang, J. Salzman, and A. Yariv, IEEE J. Quantum Electron. **QE-22**, 463 (1986).

[11]H. Kogelnik, Appl. Opt. **4**, 1562 (1965).

[12]A. P. Bogatov, P. G. Eliseev, O. G. Okhotnikov *et al.*, Kvantovaya Elektron. (Moscow) **5**, 2493 (1978) [Sov. J. Quantum Electron. **8**, 1408 (1978)].

Translated by A. Tybulewicz